www.czasopisma.pan.pl PAN POLSKA AKADEMIA NAUK www.journals.pan.pl

Arch. Metall. Mater. **67** (2022), 2, 653-659

DOI: https://doi.org/10.24425/amm.2022.137802

A.B. POP[1], A.V. SANDU[2,3], A. SACHELARIE[4*], A.M. ȚÎȚU[5*]

STUDYING THE BEHAVIOR OF THE C45 MATERIAL WHEN CHANGING THE TOOL GEOMETRY USING THE FINITE ELEMENT METHOD

Machining with tool that have cutting edge radius provides components with high fatigue strength, microhardness of a large surface layer and plastic deformation. Finite element simulations of the cutting process give a better knowledge of the chip generation phenomenon, heat generation in the machining area, stress and temperature field results. This study emphasizes the true importance of the mathematical model that underlies the shape of the tool in the pre-processing steps of finite element analysis. The argument is that its achievement and definition depend on the network difficulty. This research purpose is to perform simulations series of orthogonal machining with different radius and depth of cut. In this way, conclusions on the impact of these variations on the whole cutting process were drawn. The finite element application used is Deform 2D, the Lagrange incremental method and the Johnson-Cook material model. The temperature distribution, stress distribution, von Mises stress distribution, effects on specific tool pressure and wear, and fluctuations in the cutting resistance of the tool tip and C45 workpiece were analyzed.

Keywords: finite element simulation; cutting edge radius; specific pressures; Von Misses stresses; cutting forces

1. Introduction

When machining with a tool with a cutting edge radius, the surface layer has a high hardness and plastic deformation, and components with high fatigue resistance can be obtained [1,2]. The cutting edge radius can cause stress and temperature in the layers of the machined surface, and this can exert an effect on the processed surface properties and on tool life [3,4]. In machining simulations, it is necessary to predict the physical cutting process and the stress and temperature fields [5,6]. The tool edge radius is particularly important because it results in improved tool life and the integrity of the work surface is important [7,8]. There are two analytical methods that can study and model the transformation process: Euler and Lagrange [9-11]. Two different methods can be used in these analyzes. They are called implicit and explicit integration techniques [12-14]. Based on the literature, recent studies of FEM applications include the effects and effects of edge shape on orthogonal cutting [16], the prediction of stress and temperature on machined surfaces of various materials [17,18], and the research goals of inserts. included. Forming under the influence of radius and temperature distribution of tools and parts [19] and stress distribution in orthogonal cutting using finite element simulation [20,21]. Therefore, in carrying out this study, the Lagrange incremental formulation is used to simulate the cutting process, where the shape of the tool shows the radius of the cutting edge. In this case, the workpiece can be deformed along the radius of the tool edge, which allows the most accurate simulation of the physical chip generation process [22].

2. Research methodology

The study of bibliographic material led to the identification of some shortcomings. They hope that it will be analyzed and explained to some extent in their own research. We will also explain the implementation of the simulation of changes in the cutting edge radius and the effects of depth of cut. Cutting tool profiles were parametrically modeled using Autodesk INVENTOR and tool shape simulations were performed using DEFORM 2D.

[1] TECHNICAL UNIVERSITY OF CLUJ-NAPOCA, NORTH UNIVERSITY CENTER OF BAIA MARE, 62A, VICTOR BABEŞ STREET, BAIA MARE, ROMANIA
[2] GHEORGHE ASACHI TECHNICAL UNIVERSITY, FACULTY OF MATERIALS SCIENCE AND ENGINEERING, BLVD. D. MANGERON 71, 700050 IASI, ROMANIA
[3] ROMANIAN INVENTORS FORUM, STR. SF. P. MOVILA 3, 700089 IASI
[4] GHEORGHE ASACHI TECHNICAL UNIVERSITY OF IASI, FACULTY OF MECHANICAL ENGINEERING, D. MANGERON 41, 70050, IASI, ROMANIA
[5] "LUCIAN BLAGA" UNIVERSITY OF SIBIU, FACULTY OF ENGINEERING, 10 VICTORIEI STREET, SIBIU

* Corresponding authors: mihail.titu@ulbsibiu.ro, asachelarie@yahoo.com

3. Defining the tool and the workpiece geometry

First, we must define and model the geometry of the tool. The figure 1 contains the profile of the tool and its shape parameters. Face angle B [°], back angle C [°], cutting edge radius variants. So: L1 = 3, L2 = 3, B = 10, C = 5 and R varies: (1) R = 0.05; (2) R = 0.1; (3) R = 0.2; (4) R = 0.3; (5) R = 0.4. Cutting tool profiles and part definitions occupy an important position in the discretization step and have a significant impact on the analysis results. The next step is to select the material and mashing the previously created geometric pattern.

4. Choice of tool and workpiece materials

The tool material selected from the FEA application database is uncoated metal carbide. The working material is C45. The basic material model is Johnson-Cook, which describes the stress of plastic deformation occurring in the material, considering the effects of deformation, strain rate and temperature.

5. Discretization of the geometric models of the tool and workpiece

The network structure of the tool and workpiece model assumes that it is an interconnected external node, which is further divided into a network of specific finite element numbers or numerical integration points. This operation selects the type of finite elements to be used and determines their distribution in the discretized area, leading to their number, size and shape. Figure 2 shows the working meshing. The discretization of the geometric model of the tool is presented for each variant. So, if cutting edge radius R is 0.05 mm the model has 9794 elements and 9989 pivotal points, when R is 0.1 mm the model has 9956 elements 10149 pivotal points, when R is 0.2 mm the network has 9868 elements 10058 pivotal points, when R is 0.3 mm we have 9842 elements 10029 pivotal points and when R is 0.4 mm the model has 9795 elements 9980 pivotal points.

6. Finite element simulation

The purpose of running the simulation is to investigate the effects caused by changes in the cutting edge radius and depth

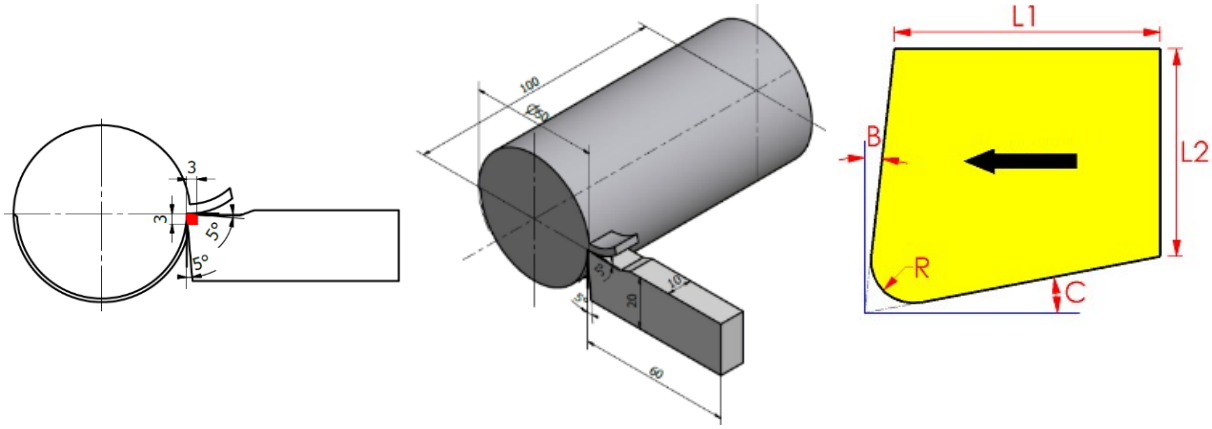

Fig. 1. Orthogonal cutting with indication of the tool tip area used in DEFORM 2D

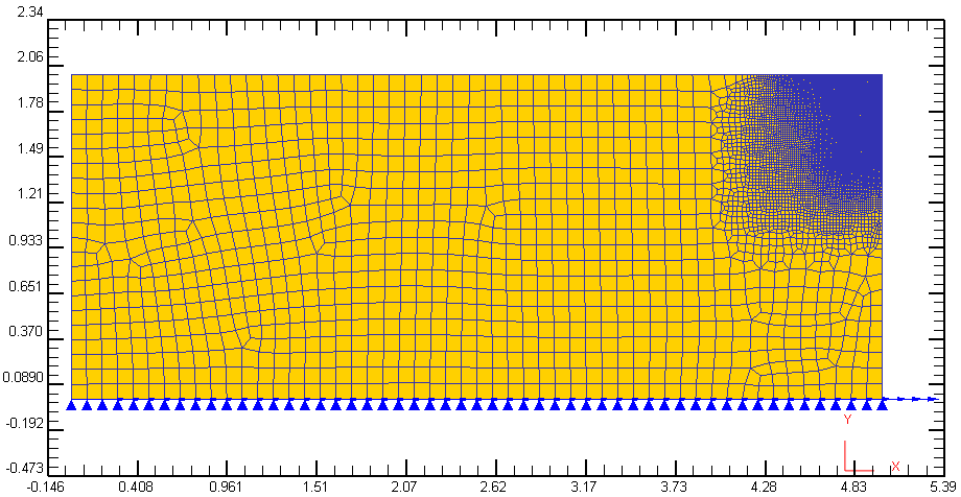

Fig. 2. Geometrical model discretization of the workpiece in a number of 10037 elements and 10217 nodes

of cut during the entire cutting process. The cutting conditions are: workpiece diameter – 50 [mm], cutting speed – 300 [m/min], feed rate – 0.1 [mm/rot], rake angle B – 10 [°], clearance angle C – 5 [°], ambient temperature – 20 [°C], tool material – uncoated carbide and the workpiece material – C45, cutting edge radius: 0.05; 0.1; 0.2; 0.3; 0.4 [mm], cutting depth; 0.3; 0.4; 0.5 [mm].

TABLE 1 shows the effective stress distribution of the workpiece over a 2 mm work surface area. The results obtained on the basis of the simulation show that the effect of the fluctuation of the cutting edge radius on the effective stress generated in the workpiece is small. The maximum values of these stresses (0.05, 0.1, 0.3 and 0.4 mm in R situations) tend to remain

TABLE 1

FEA results centralization

Cutting edge radius				
0.05 mm	**0.1 mm**	**0.2 mm**	**0.3 mm**	**0.4 mm**
Cutting depth 0.3 mm				
Effective stress [MPa] – in the workpiece – at 3 mm machining				
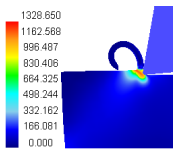	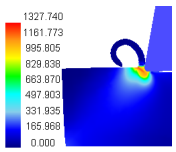	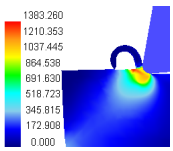	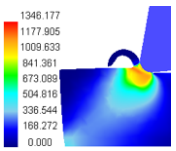	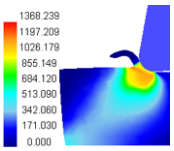
Effective stresses in the workpiece – when the tool starts the cutting process				
1328.65 MPa	1327.74 MPa	1317.95 MPa	1322.04 MPa	1340.79 MPa
Distributionof von Mises stresses in the workpiece – at 3 mm machining				
6.387 mm/mm	7.543 mm/mm	8.580 mm/mm	8.928 mm/mm	8.921 mm/mm
Workpiece temperature distribution				
643.246°C	770.743°C	885.217°C	906.460°C	909.729°C
Tool temperature distribution				
654.614°C	542.147°C	614.844°C	666.264°C	741.428°C
Cutting depth 0.4 mm				
Effective stress [MPa] – in the workpiece – at 3 mm machining				
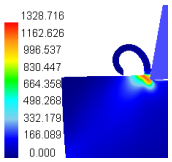	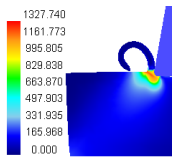	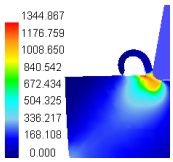	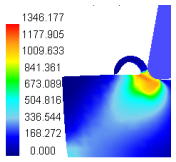	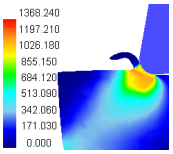
Effective stresses in the workpiece – when the tool starts the cutting process				
1328.72 MPa	1327.74 MPa	1317.95 MPa	1322.05 MPa	1340.80MPa
Distributionof von Mises stresses in the workpiece – at 3 mm machining				
6.006 mm/mm	7.521 mm/mm	8.910 mm/mm	8.924 mm/mm	8.606 mm/mm
Workpiece temperature distribution				
637.589°C	773.983°C	883.073°C	902.023°C	905.683°C
Tool temperature distribution				
658.876°C	539.725°C	622.823°C	685.143°C	729.200°C
Cutting depth 0.5 mm				
Effective stress [MPa] – in the workpiece – at 3 mm machining				
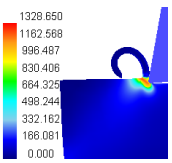	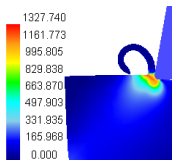	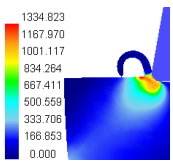	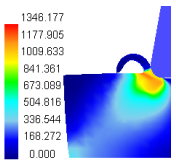	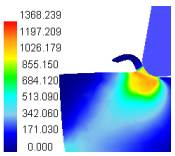
Effective stresses in the workpiece – when the tool starts the cutting process				
1328.65 MPa	1327.74 MPa	1317.95 MPa	1322.05 MPa	1340.80 MPa
Distributionof von Mises stresses in the workpiece – at 3 mm machining				
6.387 mm/mm	8.305 mm/mm	8.903 mm/mm	8.924 mm/mm	8.928 mm/mm
Workpiece temperature distribution				
643.246°C	781.321°C	879.468°C	902.023°C	916.558°C
Tool temperature distribution				
654.614°C	543.053°C	622.712°C	685.143°C	725.068°C

the same in each situation with cutting depths of 0.3, 0.4 and 0.5 mm. The same cannot be said for a cutting edge radius of 0.2 mm, because the effective stress is constantly decreasing. If the depth of cut is 0.3 mm, the maximum effective stress is 1383 260 MPa and the depth of cut is 0.4 mm. – 1344,867 MPa and 0,5 mm – 1334,823 MPa. At a cutting depth of 0.3 mm, the maximum effective stress does not show a constant increase or decrease. Here the tendencies of every simulation oscillate. However, this cannot be determined for cutting depths of 0.4 mm and 0.5 mm, as the maximum effective stress associated with the radii of 0.05 mm and 0.1 mm shows a steady decrease from 0.1 to 0.4. mm This trend is vibration-free growth in both situations (depths of cut are 0.4 and 0.5).

When the tool begins to rotate, TABLE 1 also shows that the value of the effective stress distribution of the workpiece is not directly affected by increasing the radius of the cutting tool. The data in TABLE 1 show also the vibrational values of the von Mises stress distribution with increasing changes in depth of cut. A constant increase in the value of von Mises stress is observed if the cutting edge radius increase.

According to the results in TABLE 1 from the simulation of the temperature distribution in the machining area, the change in radius is followed by an increase in temperature from 643°C to approximately 909°C – at a cutting depth of 0.3 mm. From 637°C to about 905°C when the depth of cut is 0.4 mm. From 643°C to about 916°C when the depth of cut is 0.5 mm. The effect of this tool diameter is always noticeable as the depth of cut increases. When the radius of the blade changes from 0.05 mm to 0.4 mm, the temperature gradually rises. Even in such a situation, the effect of the change in depth of cut is not felt due to the temperature value that appears on the workpiece during cutting. For example, when changing the cut, consider the radius of the cutting edge. Depth 0.3 to 0.4 and 0.5 mm – tends to remain constant. The tool temperature rises in certain zones. Therefore, in addition to the geometry of the tool, which tends to compress the material, temperature also favors it.

The graph in TABLE 2 shows the temperature ranges that occur in the turning process for the three depths of cut variations examined. For the temperature inside the tool, you can see that the temperature changes are similar in the same time interval at each depth of cut of 0.3, 0.4, 0.5 mm. For each value that the depth of cut receives, corresponding to cutting edge radii of 0.05 mm and 0.1 mm, the temperature that appears on the tool shows a steady increase. As the cutting edge radius changes (ie 0.2, 0.3, 0.4 mm), the temperature fluctuates as the value assigned to the radius increases. Regardless of the value assigned to the depth of cut, the tool tip temperature value increases as the change in radius of the cutting edge of the assigned value of 0.05, 0.1, 0.2, 0.3 and 0.4 mm increases. In the same time interval below a radius of 0.05 mm, it is observed that the temperature suddenly rises to 600°C in 0.000042 seconds. At this point, the temperature tends to normalize, its vibrations decrease, and the simulation ends. It can be seen from the graph that the higher the value assigned to the cutting edge radius, the larger the time interval in which the test moments for temperature normalization increase, and the greater the vibrations. Detailed results are shown in TABLE 3 for specific pressure distributions. An increase in the change in cutting edge radius observes an

TABLE 2

Graphical representation of the influence of the cutting-edge radius variation according to the cutting depth on the temperatures during the cutting process

Temperatures occurred in the tool	Cutting edge radius 0.05 Cutting edge radius 0.1 Cutting edge radius 0.2 Cutting edge radius 0.3 Cutting edge radius 0.4	**Temperatures occurred in the workpiece**
Cutting depth 0.3 mm	Cutting depth 0.4 mm	Cutting depth 0.5 mm
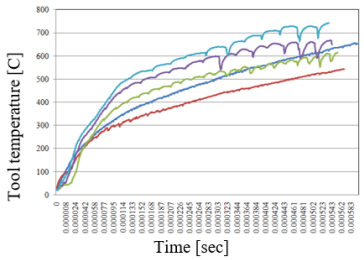	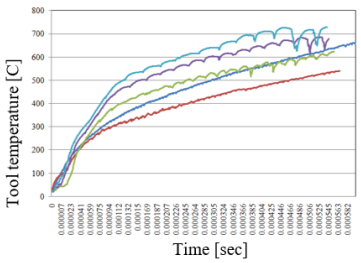	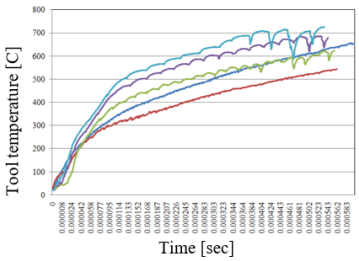
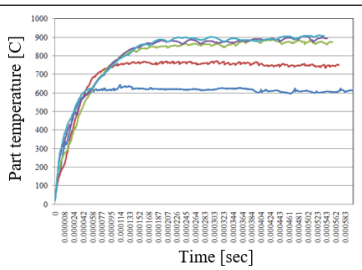	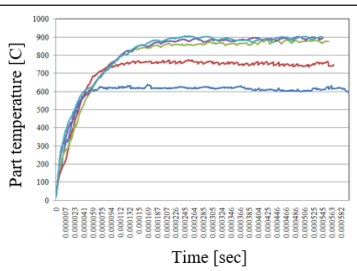	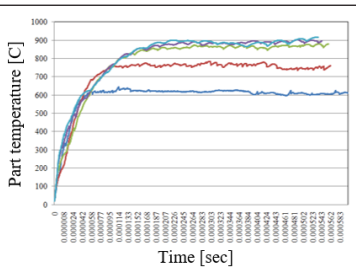

TABLE 3

Specific pressures distribution at the tool-workpiece interface

Cutting edge radius				
0.05 mm	**0.1 mm**	**0.2 mm**	**0.3 mm**	**0.4 mm**
Cutting depth 0.3 mm				
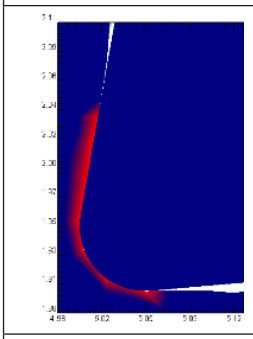	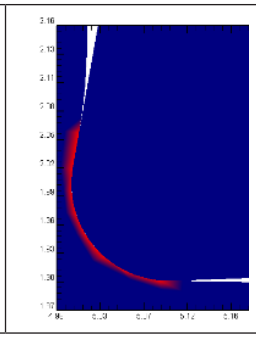	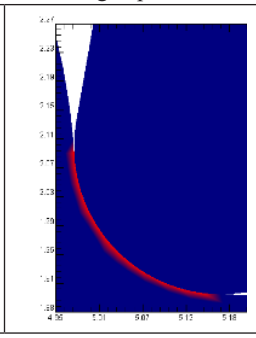	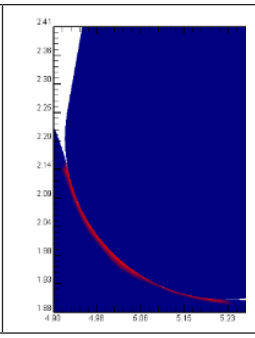	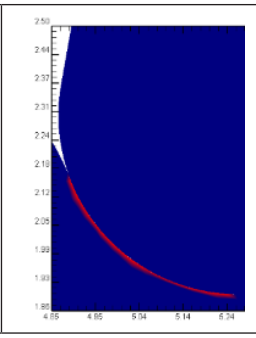
Cutting depth 0.4 mm				
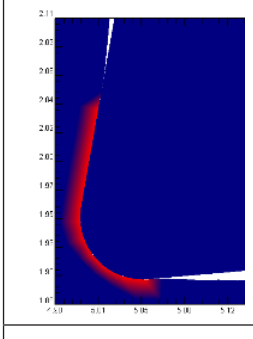	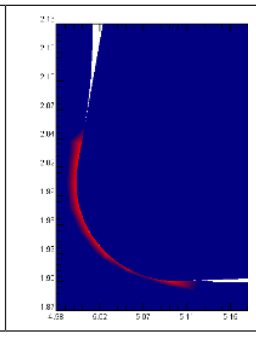	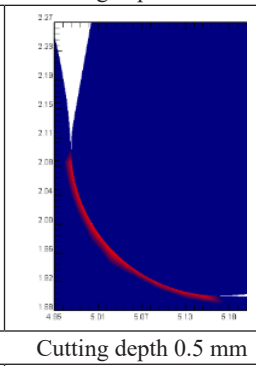	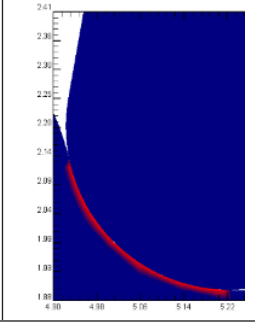	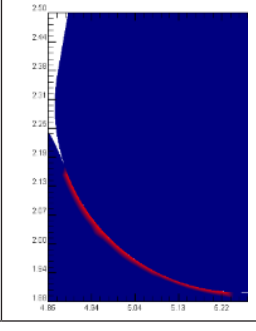
Cutting depth 0.5 mm				
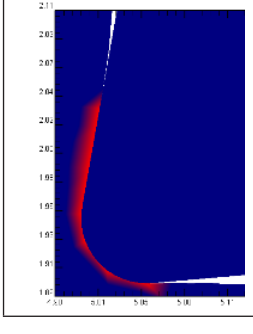	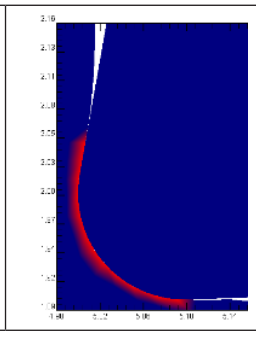	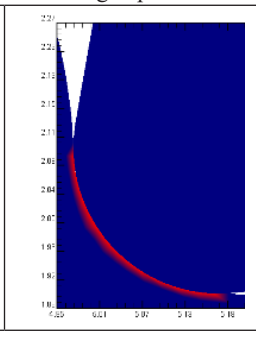	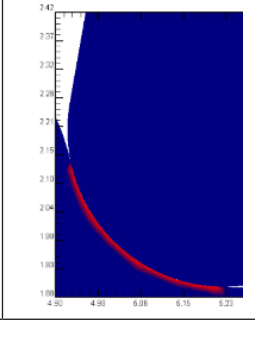	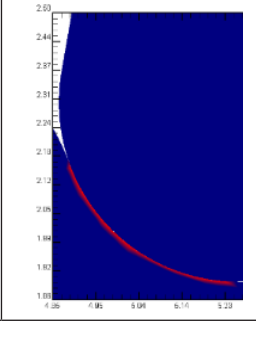

increase in these pressure distributions at the tool-part interface. As a result of this table, the X-axis contact area between the tool and the workpiece increases with a surface area of 5.06 mm, from a cutting edge radius of 0.05 mm to 0.4 mm to about 5.25 mm. At the same time, on the Y axis, which covers an area of 2.05 mm with a cutting edge radius of 0.05 mm, it will occupy an area of 2.17 mm as the radius increases when the cutting edge radius reaches 0.4. Hmm. Therefore, in situations where it is desirable to have the smallest possible specific level of pressure distribution at the interface between the tool and the workpiece, it is advantageous to reduce the value of the cutting edge radius.

The representations in TABLE 4 show the areas where tool wear occurs. The larger the sharp radius of the wheel, the larger the friction surface between the tool and the workpiece and the greater the resistance of the tool edge. The illustrations in TABLE 4 show the X and Y dimensions of the area where the wear craters occur on the free surface and its afferent positions (marked in red). Another important aspect to be analyzed is the effect of changes in the cutting edge radius on the cutting resistance with respect to the depth of cut. It is quite clear in TABLE 5 that the cutting forces generated by the cutting process show higher values at higher radii. The simulation results are displayed in the same time frame as shown below. If the cutting edge radius is small (0.05 mm), the cutting resistance increases sharply to about 200 N at the beginning of the cut, which is then maintained. As the cutting radius increases, so does the value of the cutting resistance, which is maintained for shorter and shorter time intervals, then the value of the cutting resistance increases again and renormalizes. The situation changes slightly when the depth of cut is changed from 0.3 mm to 0.4 mm and 0.5 mm. According to the figure, the cutting resistance increases slightly with increasing depth of cut. Thus, if the goal is to achieve the lowest possible cutting resistance during cutting, the preferred situation associated with the simulation data is to have the lowest cutting edge radius. The larger the cutting edge radius, the greater the effect on the cutting forces.

TABLE 4

Graphics of the tool wear

Cutting edge radius				
0.05 mm	**0.1 mm**	**0.2 mm**	**0.3 mm**	**0.4 mm**
Cutting depth 0.3 mm				
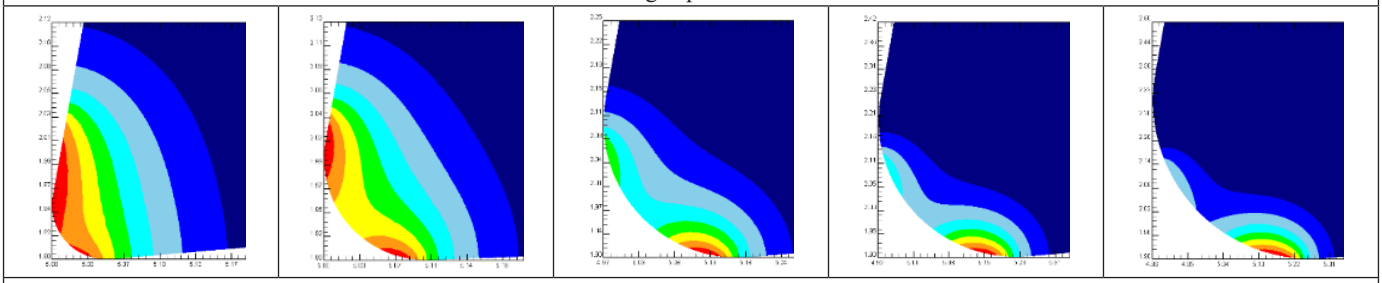				
Cutting depth 0.4 mm				
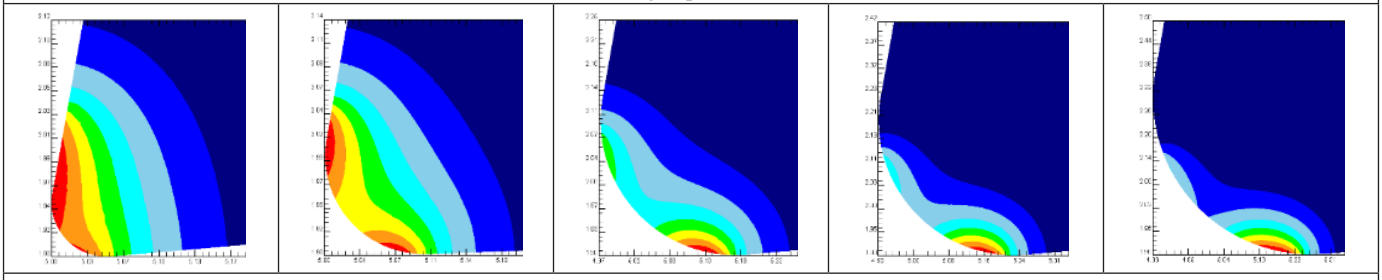				
Cutting depth 0,5 mm				
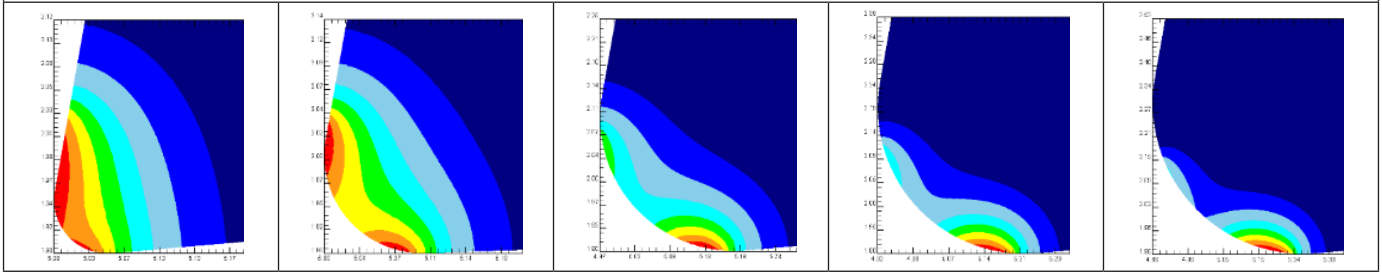				

TABLE 5

Graphical representation of the influence of R variation depending on the cutting depth on the cutting forces

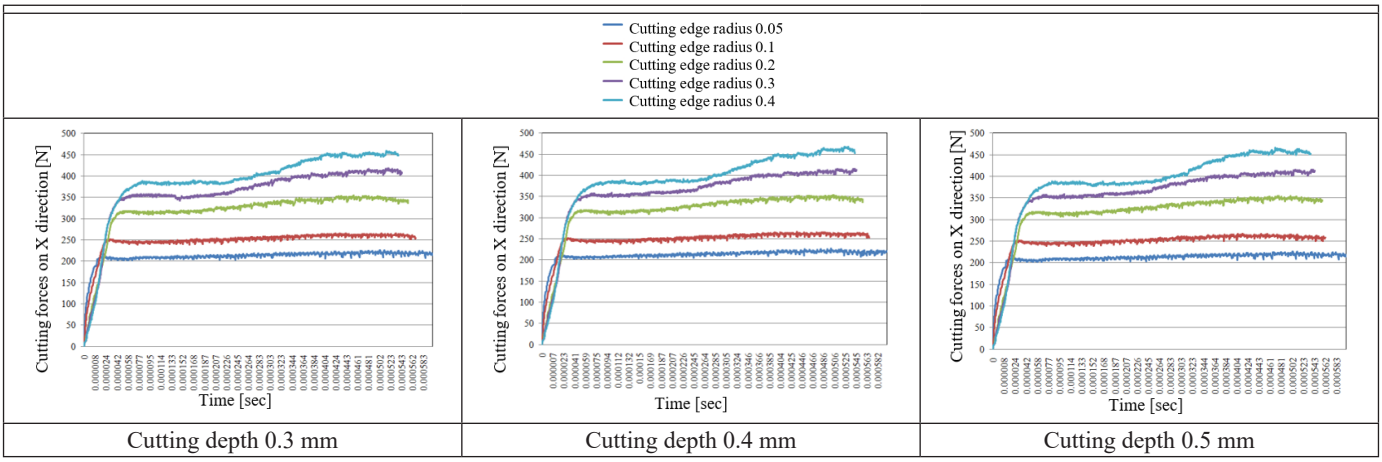

Cutting depth 0.3 mm	Cutting depth 0.4 mm	Cutting depth 0.5 mm

7. Conclusion

The change in the cutting edge radius due to the depth of cut has no significant effect, with the exception of a cutting edge radius of 0.2 mm, which reduces the tendency of the effective stress value. The stress results obtained after the section simulation show that the effective stress in the section area increases to about 1368 MPa in the same examination process by examining the effect of depth of section with increasing cutting edge radius. conditions. At the same time, the following aspects can be observed – increasing the radius of the cutting edge causes the stress distribution to radiate over a larger surface of the workpiece.

Increasing the cutting edge radius also affects the chip thickness, leading to different chip shapes, and the stress distribution of the workpiece is directly affected by the geometry of the tool tip. The depth of cut depends on the change in the radius of the cutting edge with respect to the effective stress distribution of the workpiece at the start of the tool cutting process. These rms stress values remain constant for each set of simulations for each cutting edge radius and are not a problem. Due to the values of stress vibrations in these situations, the effect of changes in the cutting edge radius due to changes in depth of cut on these stresses is also not relevant. In the von Mises stress distribution in the sense that these stress values reach approximately 8.9 mm/mm as the radius increases, only the effect of changes in the cutting edge radius is felt, not the effect of changes in the depth of cut. If the cutting edge radius changes between 0.05 and 0.4 mm, the temperature gradually increases. It can be stated based on the obtained results and the argument that the radius of the tool edge influences the temperature that occurs during cutting. Future research will be directed towards the study based on "design of experiment" through which we can get response surfaces, with applications in choosing the parameters of cutting tools. Another research direction can be considered a comparation between turning simulation results and experimental data results which conduct to highlight the simulation limits and can suggest simulation software's possibilities for improvement.

REFERENCES

[1] P.J. Arrazola, P. Aristimuno, D. Soler, T. Childs, CIRP Annals. **64**, 1, 57-60 (2015).

[2] M. Sadeghifar, R. Sedaghati, W. Jomaa, V. Songmene, Int. J. Adv. Manuf. Technol. **94**, 2457-2474 (2018).

[3] R.F. Garcia, E.C. Feix, H.T. Mendel, A.R. Gonzalez, A.J. Souza, J. Braz. Soc. Mech. Sci. Eng. **41**, 317 (2019).

[4] P.J. Arrazola, T. Özel, D. Umbrello, M. Davies, I.S. Jawahir, CIRP Annals. **62** (2), 695-718 (2013).

[5] A. Attanasio, A. Abeni, T. Özel et al., Int. . Adv. Manuf. Technol. **100**, 25-35 (2019).

[6] O.D. Yılmaz, S.N.B. Oliaei, Simulation Modelling Practice and Theory. **104**, 102-105 (2020).

[7] A. Attanasio, E. Ceretti, A. Fiorentino, A. Cappellini, C. Giardini, Wear **269**, 5-6, 344-350 (2010).

[8] M. Javidikia, M. Sadeghifar, V. Songmene et al., Int. J. Adv. Manuf. Technol. **110**, 2669-2683 (2020).

[9] M. Javidikia, M. Sadeghifar, V. Songmene, M. Jahazi, Int. J. Adv. Manuf. Technol. **106**, 4547-4565 (2020).

[10] M. Bermingham, G. Wang, M. Dargusch, SME. J. Manuf. Sci. Eng. **135**, 6, 061014 (2013).

[11] M. Calamaz, D. Coupard, F. Girot, International Journal of Machine Tools and Manufacture **48**, 3-4, 275-288 (2008).

[12] D. Cui, D. Zhang, B. Wu, M. Luo, Int. J. Mech. Sci. **131**, 613-624 (2017).

[13] M.S. Saez-de-Buruaga, D. Soler, P.X. Aristimuño, J.A. Esnaola, P.J. Arrazola, Appl. Therm. Eng. **145**, 305-314 (2018).

[14] DEFORM. Deform-User Manual. Scientific Forming Technologies Corporation (2011).

[15] Y.B. Guo, C.R. Liu, Journal of Manufacturing Science and Engineering **124**, 2, 189-199 (2002).

[16] G. List, G. Sutter, X. Bi, A. Molinari, A. Bouthiche, Journal of Materials Processing Technology **213**, 5, 693-699 (2013).

[17] J. Mackerle, Journal of Materials Processing Technology **86**, 17-44 (1999).

[18] J.C. Outeiro, P. Lenoir, A. Bosselut, Production Engineering **9**, 4, 551-562 (2015).

[19] A.K. Parida, K. Maity, Eng. Sci. Technol. and Int. J. **20**, 2, 687-693 (2017).

[20] T. Pottier, G. Germain, M. Calamaz, A. Morel, D. Coupard, Experimental Mechanics **54**, 6, 1031-1042 (2014).

[21] A.I. Jumare, K. Abou-El-Hossein, L.N. Abdulkadir, M.M. Liman, Int. J. Adv. Manuf. Technol. **103**, 4205-4220 (2019).

[22] M. Sadeghifar, M. Javidikia, V. Songmene, M. Jahazi, Simul. Model Pract. Theory **104**, 102-141 (2020).